PB82-128588

Calcium Ion Efflux Induction in Brain Tissue by Radio-Frequency Radiation

(U.S.) Health Effects Research Lab.
Research Triangle Park, NC

Prepared for

Experimental Biology Div

Sep 81

U.S. Department of Commerce
National Technical Information Service
NTIS.

TECHNICAL REPORT DATA
(Please read Instructions on the reverse before completing)

1. REPORT NO. EPA-600/S-80-082	2. BOOK ARTICLE	3. AI PB82-128588
4. TITLE AND SUBTITLE CALCIUM ION EFFLUX INDUCTION IN BRAIN TISSUE BY RADIO-FREQUENCY RADIATION		5. REPORT DATE September 1981 6. PERFORMING ORGANIZATION CODE 317042
7. AUTHOR(S) C.F. BLACKMAN, W.T. JOINES, AND J.A. ELDER		8. PERFORMING ORGANIZATION REPORT NO.
9. PERFORMING ORGANIZATION NAME AND ADDRESS Experimental Biology Division Health Effects Research Laboratory US Environmental Protection Agency Research Triangle Park, NC 27711		10. PROGRAM ELEMENT NO. ACGF1A 11. CONTRACT/GRANT NO.
12. SPONSORING AGENCY NAME AND ADDRESS Office of Research and Development (RTP,NC) Health Effects Research Laboratory US Environmental Protection Agency Research Triangle Park, North Carolina 27711		13. TYPE OF REPORT AND PERIOD COVERED 14. SPONSORING AGENCY CODE EPA-600/11

15. SUPPLEMENTARY NOTES

Published In: Biological Effects of Nonionizing Radiation, Chapter 17, 1981

16. ABSTRACT

One of the most interesting and controversial papers on the biological effects of nonionizing radiation was published by Bawin, Kaczmarek and Adey in 1975 (1). They found a 147 MHz carrier wave could elicit an enhance efflux of calcium ions from chick brain tissue only when amplitude modulated at certain sub-ELF frequencies. In addition to being one of the few U. S. reports at that time which described a biological response to an exposure at a power below 10mW/cm^2, the results demonstrated a modulation frequency-specific response with a maximum effect at 16 Hz. This response was particularly significant because the effective modulating frequencies were within the range of frequencies found in the electroencephalogram (EEG) of the intact animal.

An important feature of the research was the relatively simple biological procedure: halves of chick brains were labeled with a radioisotope ($^{45}Ca^{++}$), exposed to RF fields for a short time, and the amount of $^{45}Ca^{++}$ released into the medium during irradiation was measured. In 1979, we reported our success in replicating the essential characteristics of the frequency response curve (2). However, success was achieved only after exploring a range of power densities at 147 MHz carrier frequency, 16 Hz amplitude modulation. This result demonstrated the existence of a power density window at 0.83 mW/cm^2 in that no enhanced calcium efflux was found at either higher or lower power densities. Subsequent to this work, we examined the effect of 9 Hz modulation on the power density response and found that the location of the window was unchanged (3).

17. KEY WORDS AND DOCUMENT ANALYSIS

a. DESCRIPTORS	b. IDENTIFIERS/OPEN ENDED TERMS	c. COSATI Field/Group

REPRODUCED BY
NATIONAL TECHNICAL
INFORMATION SERVICE
U.S. DEPARTMENT OF COMMERCE
SPRINGFIELD, VA 22161

18. DISTRIBUTION STATEMENT RELEASE TO PUBLIC	19. SECURITY CLASS (This Report) UNCLASSIFIED	21. NO. OF PAGES
	20. SECURITY CLASS (This page) UNCLASSIFIED	22. PRICE

EPA-600/S-80-082
Speech

17

Calcium Ion Efflux Induction in Brain Tissue by Radiofrequency Radiation

C. F. BLACKMAN, W. T. JOINES, and J. A. ELDER

Experimental Biology Division, Health Effects Research Laboratory,
U.S. Environmental Protection Agency, Research Triangle Park, NC 27711

One of the most interesting and controversial papers on the biological effects of nonionizing radiation was published by Bawin, Kaczmarek and Adey in 1975 (1). They found a 147 MHz carrier wave could elicit an enhanced efflux of calcium ions from chick brain tissue only when amplitude modulated at certain sub-ELF frequencies. In addition to being one of the few U. S. reports at that time which described a biological response to an exposure at a power density below 10 mW/cm^2, the results demonstrated a modulation frequency-specific response with a maximum effect at 16 Hz. This response was particularly significant because the effective modulating frequencies were within the range of frequencies found in the electroencephalogram (EEG) of the intact animal.

An important feature of the research was the relatively simple biological procedure: halves of chick brains were labeled with a radioisotope ($^{45}Ca^{++}$), exposed to RF fields for a short time, and the amount of $^{45}Ca^{++}$ released into the medium during irradiation was measured. In 1979, we reported our success in replicating the essential characteristics of the frequency response curve (2). However, success was achieved only after exploring a range of power densities at 147 MHz carrier frequency, 16 Hz amplitude modulation. This result demonstrated the existence of a power density window at 0.83 mW/cm^2 in that no enhanced calcium efflux was found at either higher or lower power densities. Subsequent to this work, we examined the effect of 9 Hz modulation on the power density response and found that the location of the window was unchanged (3).

More recently, the power density response of the calcium-ion efflux at 50 MHz, modulated at 16 Hz, was examined (4). In comparison to the above results, two power-density windows were found, both of which occurred at higher exposure fields than the single effective power density at 147 MHz. With a carrier frequency of 450 MHz, Sheppard et al. (5) located a power density window that occurred within the general power

density range shown to be effective in producing calcium-ion efflux at the 147 MHz carrier frequency.

These results led us to analyze the relationship between carrier-wave frequency and power density. We developed a mathematical model (6) which takes into account the changes in complex permittivity of brain tissue with frequency. This model predicted that a given electric-field intensity within a brain-tissue sample occurred at different exposure levels for 50-, 147-, and 450-MHz radiation. Using the calculated electric-field intensities in the sample as the independent variable, the model demonstrated that the RF-induced calcium-ion efflux results at one carrier frequency corresponded to those at the other frequencies for both positive and negative findings. In this paper, we present two additional experiments using 147-MHz radiation which further test both negative and positive predictions of this model.

In addition to highlighting the basic results of the mathematical analysis outlined above, this paper presents the results of some important ancillary findings. Oxygen consumption of the sample was measured as an indication of the physiological state of the brain tissue. Requirements for certain components in the exposure medium are emphasized. Finally, we discuss mechanisms that may be responsible for the RF-induced calcium-ion efflux from brain tissue.

Experimental Procedures

The experimental procedures have been described in detail (3,4), but are briefly described here for completeness. Chick forebrains were removed, separated at the midline, and incubated at 37°C in a physiological buffer containing radioactive calcium ions ($^{45}Ca^{++}$). Any radioactivity not tightly associated with the tissue was then removed by rinsing and the samples (one forebrain half per tube) were placed in fresh buffer (1.0 ml) without the radioactive tracer. Following a 20 minute treatment in a stripline exposure system, an aliquot of the bathing solution was removed from each tube and assayed for the amount of radioactive calcium that was released from the tissue. Forebrain halves from the same chicken served as a treatment/control pair to simplify the subsequent statistical analysis. Two treatment conditions were compared in order to reduce the influence of data variability: exposure of tissue samples to radiation was alternated within a one hour period with identically prepared samples which were exposed to zero power density radiation (sham exposure). This experimental design substantially increased the sensitivity of the test. For example, the results of our previous study (2) were repeated with a much higher level of statistical significance (3), i.e. $p<.001$ compared to $p<.05$.

A detailed description of the exposure system is presented elsewhere (3). Either 50-MHz or 147-MHz radiation, sinusoidually amplitude modulated (>95%) at 16 Hz, was used to treat the samples. During treatment, the samples were maintained in a 37°C environment. In new experimental results presented here, chick forebrains were exposed at 0.37 and 0.49 mW/cm^2 to 147-MHz radiation, modulated at 16 Hz.

In an ancillary experiment, the influence of the buffering agent was tested on the ability of modulated 147-MHz radiation to enhance calcium-ion efflux. The standard medium used for these experiments was composed of 155 mM NaCl, 5.6 mM KCl, 2.16 mM $CaCl_2$, 11.1 mM glucose, and 2.4 mM $NaHCO_3$, at a pH of 7.6 to 7.8. Two other media were used, which were identical to the standard medium except for the replacement of $NaHCO_3$ with either 10 mM Tris (pH 7.4) or 10 mM HEPES (pH 7.4). The labeling, washing and exposure of the tissues were all done in medium with the same buffering agent. Exposures were conducted using 147 MHz, sinusoidally, amplitude modulated at 16 Hz, at a power density of 0.83 mW/cm^2.

The respiratory activity of the brain tissue was determined by measuring the rate of oxygen uptake with a Clark oxygen electrode (7). The sample of tissue (a brain half) was treated exactly as if used in a calcium efflux experiment except no radioactivity or RF power was used. Following this procedure which required about 55 minutes, the tissue was placed in the oxygen electrode cell containing 1.6 ml of the standard medium (pH 7.8) at 37°C and the rate of oxygen uptake was recorded.

Theoretical and Experimental Results

Outline of Mathematical Analysis. We have described the basis for the mathematical model in detail elsewhere (6). The brain tissue plus buffer was assumed to approximate a spherical object in order to simplify the mathematical development. This assumption is reasonable because the tissue rests in the hemispheric portion of the test tube (Figure 1).

Several mathematical relationships have been developed using the vector electric field intensity induced inside a sphere as a function of the incident electric field intensity (8,9). The square of the average internal electric field intensity, $|\bar{E}|^2_{av}$, was derived and related to the time-average power density incident upon the sample within the stripline. A relationship was then developed that defines the power densities at various carrier frequencies which would give the same average internal electric field intensity in the sample. These developments were necessary because the relative complex permittivity of the tissue and the wavelength of radiation change with carrier frequency. Finally, using the complex permittivity values reported by Foster et al. (10), relationships were derived for incident power densities at 50, 147,

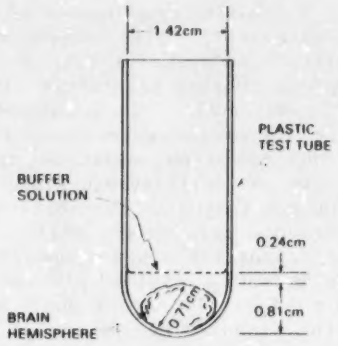

Figure 1. Schematic of the brain tissue in buffer at the bottom of the test tube used in our experiments. The mean height from the top of the tissue to the surface of the solution is 0.24 cm, and the meniscus of the solution is essentially flat across the entire diameter.

Table I. Values of P_i used in previously reported experiments on calcium-ion efflux from chick-brain samples at carrier-wave frequencies of 50, 147, and 450 MHz. The P_i values in each horizontal row are related by Equations (3) and (4) to yield the same average electric field intensity within the sample, as shown in the last column. Values of P_i yielding statistically significant results are bracketed by solid bars, cross-hatched bars bracket insignificant results, and untested values of P_i are not bracketed.

50 MHz	147 MHz	450 MHz	$\|E\|_{av}$, V/m
0.37	0.08	0.03	0.79
0.49	0.11	0.04	0.91
0.72	0.16	0.05	1.10
1.44	0.32	0.11	1.56
1.67	0.37	0.12	1.68
2.17	0.49	0.16	1.92
2.45	0.55	0.18	2.04
3.64	0.83	0.28	2.50
4.32	0.97	0.32	2.71
4.95	1.11	0.37	2.90
6.15	1.38	0.46	3.23
7.40	1.66	0.55	3.54
13.4	3.00	1.00	4.77
26.8	6.00	2.00	6.75
66.9	15.0	5.00	10.7

and 450 MHz to give the same internal electric field intensity. To augment the theoretical development and for later reference, some of the mathematical relationships are concisely stated in the following sub-section.

Equivalent Incident Power Densities at Different Frequencies. The average electric field intensity squared that is induced within a spherical sample of radius (a) much less than the wavelength (λ) of the radiofrequency field in air is

$$|\tilde{E}|^2_{av} = \left|\frac{3}{2+\varepsilon^*_r}\right|^2 E_o^2 + 0.1\,(\frac{2\pi a}{\lambda})^2\, E_o^2 \qquad (1)$$

where

$$\varepsilon^*_r = \frac{\varepsilon}{\varepsilon_o} - j\,\frac{\sigma}{\omega\varepsilon_o}$$

is the relative complex permittivity, σ is sample conductivity, ω is the radian frequency, and $e^{j\omega t}$ time dependence is assumed for all fields. The first term in Equation (1) is due to the uniform incident electric field (E_o), and the second term is due to the uniform incident magnetic field ($H_o = E_o/\eta_o$) in the stripline, where η_o = 377 ohms, the intrinsic impedance of free space. The time-averaged power density (P_i) incident upon the sample within the stripline is

$$P_i = \frac{1}{2} E_o^2/\eta_o \qquad (2)$$

To make $|E|_{av}$ within the sample the same at different carrier frequencies, we calculate from Equations (1) and (2):

$$P_{i50} = 4.46\, P_{i147} \qquad (3)$$

and

$$P_i 147 = 3.00\, P_{i450} \qquad (4)$$

where P_{if} denotes the incident power density at carrier frequency f.

Specific values of P_i used in previously reported experiments on calcium-ion efflux from chick-brain samples are listed in Table I under the carrier wave frequency used in the experiment (3,4,11). In addition, values of P_i which result in the same $|E|_{av}$ in the sample have been calculated for the other carrier frequencies using Equations (3) and (4). For example, 3.64 mW/cm^2 at 50 MHz, 0.83 mW/cm^2 at 147 MHz, and

0.28 mW/cm^2 at 450 MHz all produce the same $|E|_{av}$, 2.50 V/m, within a spherical brain tissue sample according to our model. For the incident power densities in each horizontal row, $|E|_{av}$ is calculated and shown as the last column of Table I. As indicated in Table I, positive test results have been obtained for 3.64 mW/cm^2 at 50 MHz and 0.83 mW/cm^2 at 147 MHz, while 0.28 mW/cm^2 at 450 MHz has not been tested.

If the internal electric field intensity is indeed a common factor for equality of results at each carrier frequency, then each three P_i values in a horizontal row would be bracketed by the same symbols. Since the unbracketed P_i values have not been tested in calcium-ion efflux experiments, we predict that they will yield the same results as a tested value in the same horizontal row.

Based on the positive and negative findings at 1.67 and 2.17 mW/cm^2, respectively, at 50 MHz, further studies were performed at power densities corresponding to the same $|E|_{av}$ at 147 MHz. The predictions that exposure at 0.37 mW/cm^2 would produce a positive finding and exposure at 0.49 mW/cm^2 would produce a negative finding were confirmed by these experimental results (Table II).

Table II. Mean relative quantity of calcium ions released by brain tissue pairs as a function of exposure to 147-MHz radiation, amplitude modulated at 16 Hz.

Power density	Sham			Exposed			
mW/cm^2	n	Mean	S.E.	n	Mean	S.E.	P
0.37	32	1.079	.035	32	1.221	.057	.037
0.49	32	1.150	.044	32	1.115	.041	.568

Figure 2 displays the percent difference in mean efflux between the exposed and sham groups at different power densities of 50- and 147-MHz radiation, as well as lines connecting those power densities which would produce the same value of internal electric field intensity in the samples. These results support the mathematical model and demonstrate its usefulness in defining effective power densities over a range of carrier frequencies.

The relationship between effective power densities at different carrier frequencies can be viewed in a different manner by plotting carrier frequency versus incident power density (Figure 3). Lines connecting P_i values which produce the same internal electric field intensity at 50, 147, and 450 MHz are as shown. This figure serves to illustrate the smaller range of P_i values as carrier-wave frequency is increased from

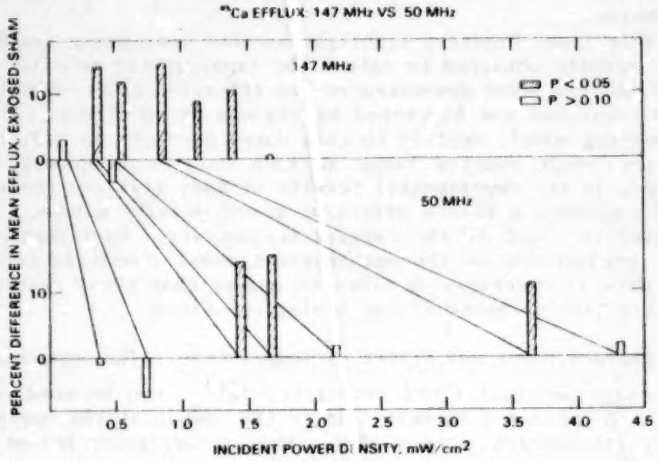

Figure 2. Percent difference in mean efflux between the exposed and sham groups vs. power density at 50 and 147 MHz. The lines connect power densities at 50 and 147 MHz, which are calculated to produce the same value of internal electric field intensity in the samples.

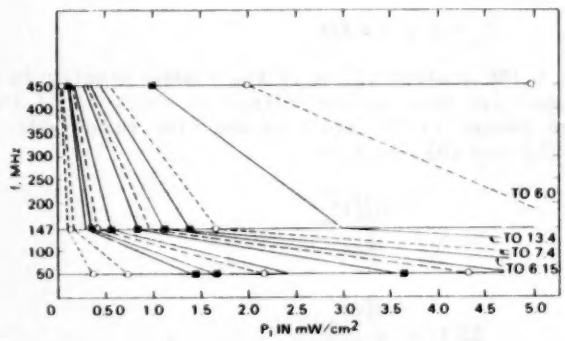

Figure 3. Results indicated in Table I at 50, 147, and 450 MHz plotted vs. P_i values (values of P_i yielding significant results (■) and insignificant results (○)). Solid and dashed lines connect P_i values that produce the same internal electric field intensity at 50, 147, and 450 MHz.

50 to 450 MHz. The implication is that better resolution between tested values of P_i should be obtained at the lower frequencies.

Table I and Figure 3 highlight another intriguing feature of the results obtained to date. The experimental results at 50 and 147 MHz have demonstrated two effective power density ranges separated and bracketed by regions of no effect. The mathematical model, applied to this data, predicts an additional effective power density range at each carrier frequency. Moreover, if the experimental results of Adey (11) are evaluated in this manner, a fourth effective power density window is predicted for each of the carrier frequencies. Confirmation of the predictions of the mathematical model resulting from these data is necessary in order to ensure that these results reflect a true response of the biological tissue.

Absorbed Power and Effect of Temperature. The square of the average internal field intensity, $|\bar{E}|^2_{av}$, can be used to compute an estimated thermal load to the sample at the various carrier frequencies. Using $|\bar{E}|^2_{av}$, the average power per unit volume absorbed within an isolated spherical sample is

$$P_a = \frac{1}{2} \sigma |\bar{E}|^2_{av} \tag{5}$$

where P_a is in W/cm^3 for σ in mhos/cm and $|\bar{E}|^2_{av}$ in V/cm. The initial slope of temperature rise within the tissue is related to P_a by

$$P_a = K \rho c \Delta T/t \tag{6}$$

where K is 4.186 joules/cal, ρ is the tissue density in g/cm^3, c is the specific heat of the tissue in cal/g°C, ΔT is the temperature change in °C, and t is the time in seconds. From Equations (5) and (6), we have

$$\Delta T/t = \frac{\sigma |\bar{E}|^2_{av}}{2K\rho c} \tag{7}$$

or

$$\Delta T/t = \frac{\sigma |\bar{E}|^2_{av}}{7.74} \tag{8}$$

taking the density and specific heat of brain tissue as 1.05 g/cm^3 and 0.88 cal/g°C (12). The use of these conservative values gives rise to an overestimate of ΔT. As an example using Equation (8), 3.64 mW/cm^2 at 50 MHz yields a $\Delta T/t$ of 3.93×10^{-7} °C/sec, and 1.00 mW/cm^2 at 450 MHz yields a $\Delta T/t$ of 2.20×10^{-6} °C/sec. Neglecting the loss of thermal energy,

the corresponding temperature rises for a 20-min exposure are 0.0005°C and 0.0026°C, respectively.

For these typical exposure conditions, the rate of energy absorption is too low to produce gross or generalized heating of the sample, or for that matter, to be measured by any readily available method. In the experiments at 147 MHz, the absorption of radiofrequency energy by the sample was so small that no difference could be detected in the amount of power incident upon the sample and the power transmitted through the exposure system. These results indicate that the effect was not due to generalized heating caused by absorption of RF energy.

In other experiments, the effect of temperature has been determined by measuring Ca^{++} efflux from chick brain tissue incubated at 32°C and 41°C (3). When compared to 37°C, the efflux was 9% lower at 32°C and 15% higher at 41°C. The temperature difference in control and irradiated samples could be experimentally controlled to less than 1°C, therefore temperature variations in the samples do not account for the 15-24% change in Ca^{++} efflux caused by exposure to 16 Hz modulated carrier waves.

Most biological effects of radiofrequency radiation are attributed to a response to the thermalized absorbed energy. However, two very important experimental results make it difficult to interpret enhanced calcium ion efflux in terms of thermal mechanisms: (a) for a given effective incident power and carrier frequency, the effect is dependent on the frequency of the modulation (1,2); and (b) there are positive-effect ranges of internal electric field intensity which are separated by no-effect regions (4). These results strongly suggest a frequency-specific phenomenon and provide evidence against gross thermal mechanisms.

Proposed Mechanism Responsible for Calcium Efflux.

Calcium-ion efflux from brain tissue does not appear to be a function of carrier frequency, since equivalent results are obtained at carrier frequencies of 50, 147, and 450 MHz provided the internal electric field intensity is the same in each brain. However, an important question remains: why should there be alternate ranges, or windows, of internal electric field intensity which cause efflux enhancement? An hypothesis that is consistent with and helps explain this finding is: The internal electric field $|E|_{av}$ in Equation (1) has a linear as well as a nonlinear dependence on the external electric field (E_o) for the specific values of E that yield enhanced efflux.

With regard to this hypothesis, only the first term in Equation (1) is a function of tissue properties, since

$$\varepsilon_r^* = \frac{\varepsilon}{\varepsilon_o} - j\frac{\sigma}{\omega\varepsilon_o}.$$

Hence, ε_r^* may have a small nonlinear dependence upon E_o. Biological membranes are known to have a nonlinear response to a static or low-frequency electric field (13,14,15), and many researchers have suggested a nonlinear response for biological materials due to RF fields (16-20). Neglecting the second term of Equation (1), the simplest linear plus nonlinear dependence of $|E|_{av}$ on E_o may be expressed as

$$|E|_{av} = k_1 E_o + k_2 E_o^2 = k_1 \left(1 + \frac{k_2}{k_1} E_o\right) E_o \tag{9}$$

where $k_1 = 3/(2 + \varepsilon_r^*)$ and k_2 is a parameter to be determined as a function of k_1 and E_o.

The external field (E_o) is a modulated carrier wave represented by

$$E_o = E_{oc} (1 + m \cos \omega_m t) \cos \omega_c t \tag{10}$$

where E_{oc} is the amplitude of the unmodulated carrier, m is the modulation index, $\omega_m/2\pi = f_m$ is the modulation frequency (typically 16 Hz), and $\omega_c/2\pi = f_c$ is the carrier frequency (typically 50, 147, or 450 MHz). Substituting Equation (10) into Equation (9), and using trigonometric identities, yields

$$|E|_{av} = k_1 E_{oc} \cos \omega_c t + k_2 E_{oc}^2 m \cos \omega_m t + \frac{k_2 E_{oc}^2}{4} (2 + m^2) +$$

$$\frac{k_1 E_{oc}}{2} m \cos (\omega_c + \omega_m) t + \frac{k_1 E_{oc}}{2} m \cos (\omega_c - \omega_m) t +$$

$$\frac{k_2 E_{oc}^2}{2} \cos 2\omega_c t + \frac{k_2 E_{oc}^2}{4} m^2 \cos 2\omega_m t +$$

$$\frac{k_2 E_{oc}^2}{2} m \cos (2\omega_c + \omega_m) t + \frac{k_2 E_{oc}^2}{2} m \cos (2\omega_c - \omega_m) t +$$

$$\frac{k_2 E_{oc}^2 m^2}{4} \cos 2\omega_c t + \frac{k_2 E_{oc}^2 m^2}{8} \cos (2\omega_c + 2\omega_m) t +$$

$$\frac{k_2 E_{oc}^2 m^2}{8} \cos (2\omega_c - 2\omega_m) t \tag{11}$$

The first term in Equation (11) is the unmodulated carrier wave, of amplitude $k_1 E_{oc}$, and the second term is a signal at the modulation frequency, of amplitude $k_2 E_{oc}^2 m$, generated by the nonlinear dependence of E on E_o.

The field intensities, or wave amplitudes, that have produced changes in calcium-ion efflux at typical carrier frequencies and at typical modulation frequencies may be used to estimate the amount of nonlinearity that would be required to conform with observed results. Adey (11) has reported that a relatively small internal electric field intensity, on the order of 10^{-7} V/cm, at 16 Hz is sufficient to alter the binding of calcium ions in brain tissue. The internal field intensity of the carrier waves shown in Table 1 are on the order of 10^{-2} V/cm. From these observations, the ratio of the amplitudes of the first two terms in Equation (11) is

$$\frac{k_2 E_{oc}^2 m}{k_1 E_{oc}} = \frac{10^{-7}}{10^{-2}} = 10^{-5} \tag{12}$$

and assuming a modulation index of m = 1,

$$\frac{k_2}{k_1} E_{oc} = 10^{-5} \tag{13}$$

By substituting 10^{-5} for $k_2 E_o / k_1$ in Equation (9), it is apparent that the suggested amount of nonlinearity is very small and would not be detectable by conventional measurements of ε_r^* versus $|E|_{av}$.

To account for the alternate ranges of effective incident power densities, the internal field $|E|_{av}$ need only have a small nonlinear dependence upon the external field (E_o) at specific values of internal electric field (E) that yield enhanced efflux. At all other values of E, the dependence of $|E|_{av}$ on E_o may be entirely linear. A plot of $|E|_{av}$ versus E_o from Equation (1), at the carrier frequencies 50, 147, and 450 MHz, is shown in Figure 4. Obviously, a deviation from linearity of the amount estimated earlier (1 part in 10,000) would not be noticed on the straight lines of Figure 4. However, the $|E|_{av}$ values where the relationship is assumed to be slightly nonlinear are indicated by the solid horizontal lines. These solid lines indicate the $|E|_{av}$ values from Table 1 which correspond to P_i (or E_o) values that produced efflux enhancement. The dashed horizontal lines in Figure 4 indicate $|E|_{av}$ values corresponding to P_i (or E_o) values that were not effective. At these points, the dependence of $|E|_{av}$ on E_o may be entirely linear. At present, we have no firm hypothesis to describe the postulated multiple regions of nonlinear dependence of the internal field, E, on the external field, E_o.

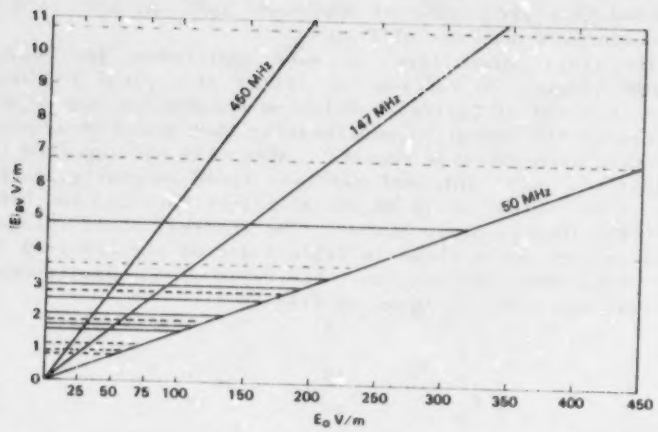

Figure 4. Average internal electric field intensity ($|E|_{av}$) as a function of the external electric field intensity (E_o) for 50-, 147-, and 450-MHz carrier frequencies.

Solid horizontal lines indicate values of $|E|_{av}$ that correspond to E_o (or P_i) values that produce efflux enhancement. The dashed horizontal lines indicate similar values where no significant enhancement of efflux has been observed.

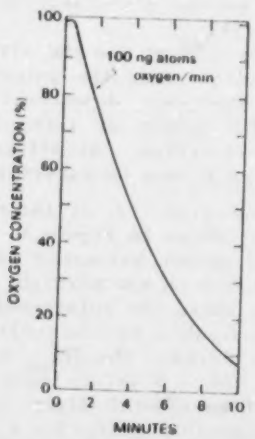

Figure 5. Respiratory activity of chick brain tissue.

A sample (brain half) was treated exactly as if used in a calcium efflux experiment except no radioactivity or RF power was used. Following this procedure, which required about 55 min, the tissue was placed in an oxygen electrode cell containing 1.6 ml. of the medium (pH 7.8) at 37° C, and the rate of oxygen consumption was measured (7, 23).

An additional hypothesis that is consistent with and helps explain the role played by the 16 Hz amplitude modulation is as follows: the nonlinear medium demodulates the carrier releasing a 16-Hz signal within the brain tissue, and it is the 16-Hz signal that causes changes in the calcium binding. This change in calcium binding may occur by Maxwell-Wagner relaxation (21) at the polarized interface between the Ca^{++} ions and the brain tissue. This hypothesis is not developed here. Alternative hypotheses have been offered (cf. Adey, this volume) to explain the fundamental role played by the sub-ELF (1,2,22). Obviously, more theoretical and experimental work must be performed before a clear choice can be made regarding the most likely hypothesis.

Ancillary Experiments

Effect of Buffer Solution. An essential component of the medium in potentiating enhanced calcium-ion efflux due to RF radiation appears to be bicarbonate. We have substituted both Tris and HEPES buffers for bicarbonate and have failed to observe enhanced calcium efflux at 0.83 mW/cm^2 (147 MHz). The same result has been reported by Bawin (personal communication) when bicarbonate was replaced by imidazole or MOPS buffers. Although the significance of this finding is not yet apparent, these results should be of interest to other investigators who attempt to replicate or extend the studies on RF-induced calcium-ion efflux from brain tissue. One should also note that the initial report by Bawin et al. (1) incorrectly listed the bicarbonate concentration at 24 mM instead of 2.4 mM (22).

Respiratory Activity of Brain. Questions concerning the metabolic state of the isolated brain tissue are frequently posed. Figure 5 shows the respiratory activity of a brain half which had undergone the same treatment as a sample used in calcium efflux experiments. The initial linear portion of the curve represents a respiratory rate of about 100 ng atoms oxygen/min. The rate decreased with time and more than 90% of the oxygen in the medium was depleted in less than 10 min. When the oxygen-depleted solution was repeatedly replaced with fresh medium, very similar curves were obtained. For example, the initial respiratory rates in the second and third replacement volumes were 6% and 15% less than the first trial, respectively. The tissue was therefore capable of respiratory activity throughout the 55 to 60 minute experimental period. Freshly excised brain samples exhibited similar responses at slightly higher respiratory rates. One should recall that Bawin et al. (1) added cyanide to the samples and found that the respiratory poison (inhibitor) did not affect enhanced calcium efflux.

Summary and Conclusion

Keeping the average electric field intensity the same within a spherical model of chick-brain in buffer solution at different incident carrier wave frequencies requires that incident power density be changed with frequency to compensate for the change in complex permittivity and wavelength with frequency. The resulting Equations (3) and (4) relate corresponding values of P_i at carrier frequencies of 50, 147, and 450 MHz.

Very few results are available to test this mathematical model. Circumstances have lead to two tests comparing a negative and a positive finding at 147 MHz with results at 450 MHz. One test was performed at 50 MHz (3.64 mW/cm^2) to test a prediction of this model based on the result of 147 MHz (0.83 mW/cm^2). All these tests have provided results that agree with the model. In this paper, we describe the results of two tests at 147 MHz which agree with the predictions, one positive and one negative, made from the 50 MHz data. Thus, all the results to date support the predictions of the theoretical analysis. Further support for the theory is the fact that no result is contradicted by a corresponding experiment at a different carrier frequency. A more complete test of the theory will be obtained when additional experiments are conducted at the untested values of P_i.

The experimental results suggest that radiofrequency radiation may be useful as an investigative tool to learn more about the electrical properties of the central nervous system.

The specific carrier-wave amplitudes (field intensities) which have been found to be effective in producing Ca^{++} ion efflux are discussed in terms of tissue properties and relevant mechanisms. The brain tissue is hypothesized to be electrically nonlinear at specific field intensities; this nonlinearity demodulates the carrier and releases a 16 Hz signal within the tissue. The 16 Hz signal is selectively coupled to the Ca^{++} ions by some mechanism, perhaps a dipolar-type (Maxwell-Wagner) relaxation, which enhances the efflux of Ca^{++} ions. The hypothesis that brain tissue exhibits a slight nonlinearity for certain values of applied RF electric field intensity is not testable by conventional measurements of ε_r^* because changes in this factor on the order of 1 part in 10,000 are not detectable. However, the Ca^{++} ion efflux experiment itself may prove to be the most sensitive and discriminating indicator to date of nonlinear electrical behavior in biological tissue. The specific values of electric field intensity where the tissue may be electrically nonlinear (e.g., 2.5 V/m) should be tested in other experiments where a tissue nonlinearity could release a low frequency or a DC signal (the third term in Equation 11) which could in turn interact with on-going biological activities.

Literature Cited

1. Bawin, S. M.; Kaczmarek, L. K.; Adey, W. R. Effects of modulated VHF fields on the central nervous system. Ann. N.Y. Acad. Sci., 1975, 247, 74-81.
2. Blackman, C. F.; Elder, J. A.; Weil, C. M.; Benane, S. G.; Eichinger, D. C.; House, D. E. Induction of calcium-ion efflux from brain tissue by radio-frequency radiation: Effects of modulation frequency and field strength. Radio Science, 1979, 14(6S), 93-98.
3. Blackman, C. F.; Benane, S. G.; Elder, J. A.; House, D. E.; Lampe, J. A.; Faulk, J. M. Induction of calcium-ion efflux from brain tissue by radio frequency radiation: Effect of sample number and modulation frequency on the power-density window. Bioelectromagnetics, 1980, 1, 35-48.
4. Blackman, C. F.; Benane, S. G.; Joines, W. T.; Hollis, M. A.; House, D. E. Calcium-ion efflux from brain tissue: Power density vs. internal field intensity dependencies at 50-MHz RF radiation. Bioelectromagnetics, 1980, 1(3).
5. Sheppard, A. R.; Bawin, S. M.; Adey, W. R. Models of long-range order in cerebral macromolecules: Effects of sub-ELF and of modulated VHF and UHF fields. Radio Science, 1979, 14(6S), 141-145.
6. Joines, W. T.; Blackman, C. F. Power density, field intensity, and carrier frequency determinants of RF-induced calcium-ion efflux from brain tissue. Bioelectromagnetics, 1980, 1(3).
7. Lessler, M. A.; Brierley, G. P. Oxygen electrode measurements in biochemical analysis. Methods Biochem. Anal., 1969, 17, 1-29.
8. Lin, J. C.; Guy, A. W.; Johnson, C. C. Power deposition in a spherical model of a man exposed to 1-20 MHz electromagnetic fields. IEEE Trans. Microwave Theory Tech., 1973, 21, 791-797.
9. Spiegel, R. J. ELF coupling to spherical models of man and animals. IEEE Trans. Biomed. Eng., 1976, 23 387-391.
10. Foster, K. R.; Schepps, J. L; Stoy, R. D.; Schwan, H. P. Dielectric properties of brain tissue between 0.01 and 10 GHz. Phys. Med. Biol., 1979, 24, 1177-1187.
11. Adey, W. R. Frequency and power windowing in tissue interactions with weak electromagnetic fields. Proc. IEEE, 1980, 68(1), 119-125.
12. Cooper, T. E.; Trezek, G. J. A probe technique for determining the thermal conductivity of tissue. J. Heat. Transfer, 1972, 94, 133-140.
13. Goldman, D. E. Potential impedance and rectification in membranes. J. Gen. Physiol., 1943, 27, 37-60.

14. Hamel, B. B.; Zimmerman, I. A dipole model for negative steady-state resistance in excitable membranes. Biophys. J., 1970, 10, 1029-1056.
15. Arndt, R. A.; Bond, J. D.; Roper, L. D. A fit to nerve membrane rectification curves with a double-dipole-layer membrane model. Bull. Math. Biophys., 1972, 34, 151-172.
16. Spiegel, R. J.; Joines, W. T. A semiclassical theory for nerve excitation by a low intensity electromagnetic field. Bull. Math. Biophys., 1973, 35, 591-605.
17. Wachtel, H.; Seaman, R. L.; Joines, W. T. Effects of low-intensity microwaves on isolated neurons. Ann. N. Y. Acad. Sci., 1975, 247, 46-52.
18. Joines, W. T. Reception of microwaves by the brain. Med. Res. Eng., 1976, 12, 8-12.
19. Barnes, F. S.; Hu, C. L. Model for some non-thermal effects of radio and microwave fields on biological membranes. IEEE Trans. Microwave Theory Tech., 1977, MTT-25, 742-746.
20. Berkowitz, G. C.; Barnes, F. S. The effects of nonlinear membrane capacity on the interaction of microwave and radio frequencies with biological materials. IEEE Trans. Microwave Theory Tech., 1979, MTT-27, 204-207.
21. Pethig, R. "Dielectric and Electronic Properties of Biological Materials"; John Wiley & Sons, New York, 1979; p. 153.
22. Bawin, S. M.; Adey, W. R.; Sabbot, I. M. Ionic factors in release of $^{45}Ca^{2+}$ from chicken cerebral tissue by electromagnetic fields. Proc. Nat. Acad. Sci. (US), 1978, 75, 6314-6318.
23. Elder, J. A.; Ali, J. S. The effect of microwaves (2450 MHz) on isolated rat liver mitochondria. Ann. N.Y. Acad. Sci., 1975, 247, 251-262.

RECEIVED December 1, 1980.

ACS SYMPOSIUM SERIES, No. 157
BIOLOGICAL EFFECTS OF NONIONIZING RADIATION
Karl H. Illinger, Editor